Computer Methods and Programs in Biomedicine xxx (xxxx) 106262

Contents lists available at ScienceDirect

Computer Methods and Programs in Biomedicine

journal homepage: www.elsevier.com

A new approach for initial callus growth during fracture healing in long bones

J.M. Naveiro [a, b], S. Puértolas [a, b, *], J. Rosell [a, b], A. Hidalgo [a], E. Ibarz [a, b], J. Albareda [c, d, e], L. Gracia [a, b]

[a] Department of Mechanical Engineering, University of Zaragoza, Zaragoza, Spain
[b] Aragón Institute for Engineering Research, Zaragoza, Spain
[c] Department of Surgery, University of Zaragoza, Zaragoza, Spain
[d] Aragón Health Research Institute, Zaragoza, Spain
[e] Hospital Clínico Universitario Lozano Blesa, Zaragoza, Spain

ARTICLE INFO

Article history:
Received 8 March 2021
Accepted 28 June 2021

Keywords:
Fracture healing
Bone callus formation
Bone growth factors
Finite element simulation
Automatic mesh generation

ABSTRACT

The incidence of bone fracture has become a major clinical problem on a worldwide scale. In the past two decades there has been an increase in the use of computational tools to analyse the bone fracture problem. In several works, various study cases have been analysed to compare human and animal bone fracture healing. Unfortunately, there are not many publications about computational advances in this field and the existing approaches to the problem are usually similar.

In this context, the objective of this work is the application of a diffusion problem in the model of the bone fragments resulting from fracture, working together with a mesh-growing algorithm that allows free growth of the callus depending on the established conditions, without a pre-meshed domain. The diffusion problem concerns the different biological magnitudes controlling the callus growth, among which Mesenchymal Stem Cells and chondrocytes concentrations were chosen, together with Tumour Necrosis Factor α and Bone Morphogenetic Protein as the factors influencing the velocity in the callus formation. A Finite Element approach was used to solve the corresponding diffusion problems, obtaining the concentration values along the entire domain and allowing detecting the zones in which biological magnitudes reach the necessary thresholds for callus growth. The callus growth is guided by a geometrical algorithm which performs an additional mesh generation process (self-added mesh) at each step of the iterative procedure until complete callus formation.

The proposed approach was applied to different types of diaphyseal femoral fractures treated by means of intramedullary nailing. Axisymmetric models based on triangular quadratic elements were used, obtaining results in good agreement with clinical evidence of these kinds of fractures.

The algorithm proposed has the advantage of a natural callus growth, without the existence of a previous mesh that may affect the conditions and direction of growth. The approach is intended for the initial phase of callus growth. Future work will address the implementation of the corresponding formulations for tissue transformation and bone remodelling in order to achieve complete fracture healing.

1. Introduction

The prevalence of bone fracture has become an increasing public health problem on a worldwide scale [1]. Even if the incidence rates were to remain stable, due to developments in health care and a higher standard of living, the occurrence of fractures would increase in any case due to the increasing number of people older than sixty-five [1]. This in turn will lead to a higher risk of people suffering bone problems such as osteoporosis, which is linked to the femur and hip fracture problem.

Since 2010, more than 250,000 bone fractures per year have been recorded in the European Union due to accidents at work [2]. More-

Abbreviations: IM, Intramedullary nail; CT, Computerized Tomography; FE, Finite Element; MSCs, Mesenchymal stem cells; BMPs, Bone morphogenetic proteins; TNF -α, Tumour Necrosis Factor α; CC, chondrocytes concentration; BMP-2, Bone Morphogenetic Protein 2

* Corresponding author at: Department of Mechanical Engineering, EINA – Engineering and Architecture School, University of Zaragoza, María de Luna, s/n (Edif. Betancourt), 50018 Zaragoza Spain.
E-mail address: spb@unizar.es (S. Puértolas).

https://doi.org/10.1016/j.cmpb.2021.106262
0169-2607/

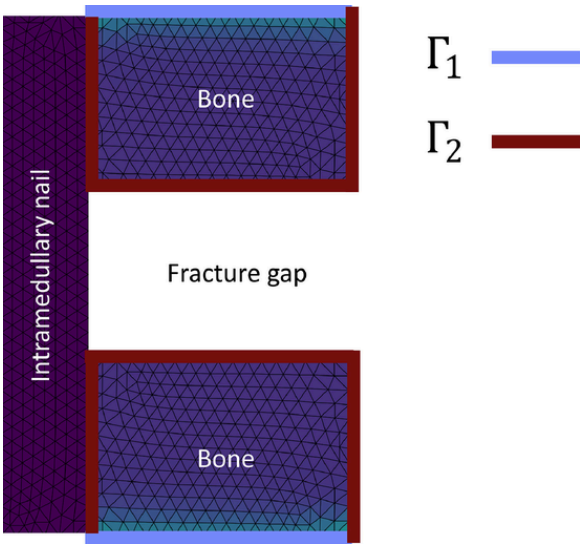

Fig. 1. Axisymmetric model of a diaphyseal femoral fracture treated by means of an intramedullary nail. Boundary Conditions of the diffusion problem: Γ_1, initial predefined concentration values, Γ_2, zero flow rate.

over, in 2010 a total of 620,000 hip fractures were recorded in the EU. Within this number, the osteoporotic fractures were associated with morbidity and mortality, and increasing social costs [3]. Fragility fractures had an estimated economic burden of 37 billion euros and accounted for almost 1.2 million quality-adjusted life years in that same year [4].

It has been estimated that during the thirty years after 2020, the number of hip fractures around the world will increase to more than two thousand million cases [5]. Hip fractures due to osteoporosis are usually accompanied by a femur fracture.

When a femur fracture occurs, a common surgical procedure is to implant an intramedullary nail (IM). This surgery is not easy and has some risks including infection, morbidity and pain [6]. These post-operative complications must be prevented with all the resources at the doctors' disposal. Research on this topic is needed to achieve better results. Radiographs, Computerized Tomography (CT) scans and all the existing tools to help the preparation for bone fracture surgery are of course necessary. However, more support tools are needed for a better understanding of how to proceed to prevent the above-mentioned problems.

At the cell scale, obtaining data related with the bone healing process is achieved by means of investigation in vivo and in vitro [7]. Such data are very difficult to obtain due to the time involved, the expensive resources required, and the difficulty in generalizing the results. Computational models have emerged as an alternative to provide extra support to the obtaining of data. Furthermore, computational models represent a powerful prediction tool.

In the past two decades, there has been an increase in the use of computational tools to analyse the bone fracture problem. Unfortunately, there are few publications about computational advances in this field. Claes et al. [8] estimated stresses and strains in a fracture callus using three finite element (FE) models applied to tissular differentiation. The first model reflects the morphology occurring one week after fracture. The second and third models describe the fourth and eighth healing weeks, respectively. To describe progressive stiffening of the callus, they assumed five tissue types differing in their elastic material properties. In the initial healing stage, the callus consisted only of connective tissue. The second model contained callus of intermediate stiffness in a small region along the periosteum, and soft callus tissue adjacent to it, while the remainder consisted of initial connective tissue. In the third model the callus tissue contained five tissue types: initial connective tissue, soft callus, intermediate stiffness callus, stiff callus and chondroid ossification zone. Consequently, there is a predefined domain for the callus and there is no mesh generation. Bailón-Plaza et al. [9] presented a two-dimensional mathematical model of the bone healing process for moderate fracture gap sizes and fracture stability, in which the inflammatory and tissue regeneration stages of healing were simulated by modelling mesenchymal cell migration. Lacroix et al. [10]

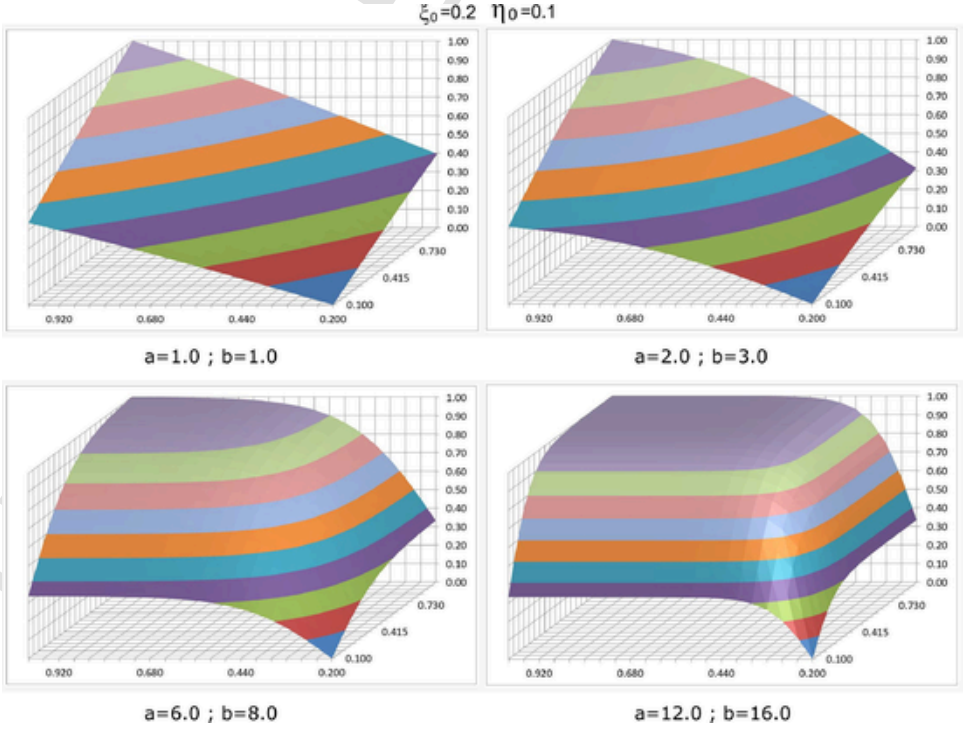

Fig. 2. Different shapes of parametric function depending on a, b values. The parameters a and b are positive constants that adjust the slopes of the function and are related to the concentrations of the considered chemical factors (in the model TNF-α and BMP-2 were used).

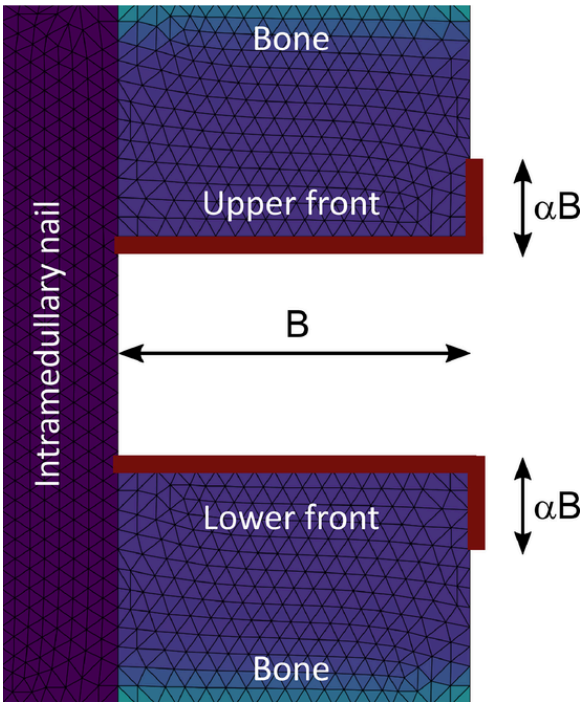

Fig. 3. Growth boundary. Location where the callus starts to grow, corresponding to free boundaries at the fracture site.

used a biphasic poroelastic FE model of a fracture callus for modelling the time course of tissue differentiation during fracture healing. Simon et al. [11] developed a dynamic model to simulate complex interactions of mechanical stability, revascularisation and tissue differentiation in secondary fracture healing. The model used an axisymmetric FE model to describe the fracture callus and fuzzy logic rules to control biological procedures. In a subsequent study, the same authors used fuzzy logic in a similar manner [12]. Cameron et al. [13] presented a FE model of a sheep tibial osteotomy comparing results with real ones. Finally, Wang et al. [14] showed a dynamic three-dimensional fracture healing model with biphasic poroelastic finite element analysis and fuzzy logic control, calculating the local biophysical stimulus and different tissue distribution within the callus. When compared with experimental observations, the model had a good prediction outcome. In this model the shape of the callus is predefined, there is no mesh generation, and the approach is tissular differentiation.

The most common approach in the published works [8-15] focuses on tissular differentiation and bone remodelling, considering a predefined callus form (pre-meshed domain), changing or updating the type of material of the elements according to the evolution of strains, stresses and fluid pressure.

The typical approach to the diffusion problem, for computational solving, considers one main variable and one or more factors affecting the velocity in the diffusion problem. The most common main variable for the diffusion problem is the Mesenchymal Stem Cells (MSCs) concentration; the growth process depends directly from the recruitment of MSCs and the biggest sources of this resource are muscles, skin, adipose tissue and bone marrow [16]. As for the factors, researchers consider Bone Morphogenetic Proteins (BMPs) as accelerators.

In biological terms, the most influential factors controlling fracture healing are the Tumour Necrosis Factor α (TNF-α) and the superfamily of Transforming Growth Factor beta (TGF-β). The TNF-α helps in the regulatory process of the immune system during the inflammatory phase [17]. Furthermore, it is present in the MSCs recruitment phase. However, its most important role occurs at the beginning of the chondrocyte apoptosis [18]. BMPs are a subfamily within the TGF-β superfamily [18], which are the most widely studied for clinical applications [17, 18]. The BMPs are osteoinductive proteins that induce bone formation, accelerate union time and prevent non-union [19].

In this context, this work presents a new approach for initial callus growth during fracture healing in long bones. The objective is the application of a diffusion model working together with a mesh growing algorithm that allows free growth of the callus depending on the established conditions, without a pre-meshed domain. Furthermore, the iterative algorithm allows the generation and step by step control of the mesh. As biological magnitudes, the chosen variables were the MSC and the chondrocyte concentrations (CC), and the factors influencing the velocity in the callus formation were the TNF-α and the Bone Morphogenetic Protein2 (BMP-2). The model allows selecting or changing the different biological and chemical magnitudes. The work is intended to simulate the initial phase of callus formation; tissue differentiation and remodeling will be addressed in future works in order to complete the simulation of the whole fracture healing process.

2. Materials and Methods

The proposed approach consists of a first phase corresponding to the diffusion problem concerning biological magnitudes that control the

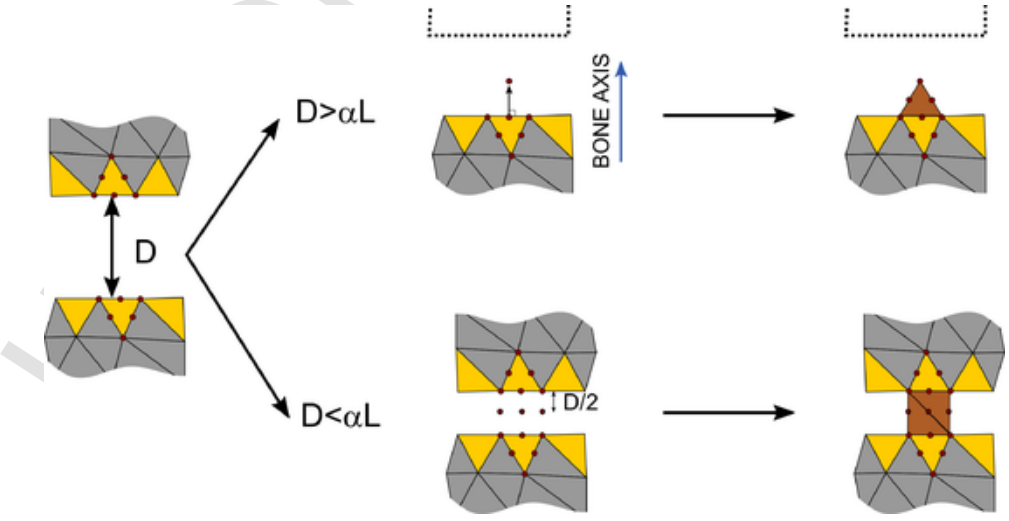

Fig. 4. How the callus growth algorithm works. When the distance between lower and upper fronts is higher than α times the average mesh size (L), there is a normal triangular growth. When the distance is lower, the two fronts close with two triangles forming a square.

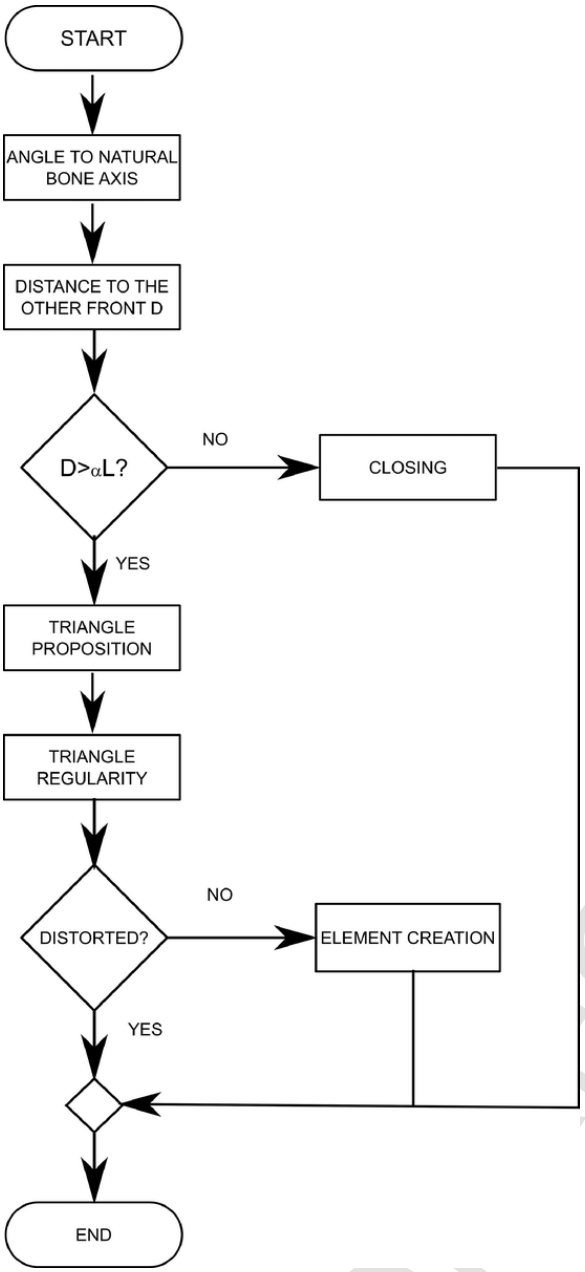

Fig. 5. Flow chart of the growth algorithm.

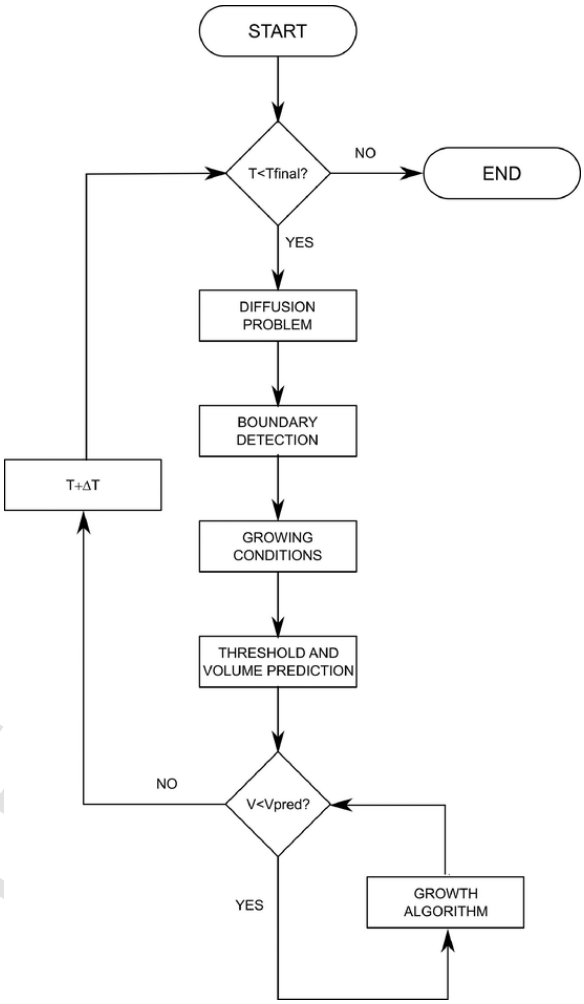

Fig. 6. Flow chart of the complete process.

callus formation, numerically solved by means of the appropriate finite element formulation, together with a second phase in which a specific algorithm performs the mesh growth in the case that the biological magnitudes reach the prescribed thresholds. Then, both phases work in conjunction in an iterative process until callus formation is complete. The approach is applied to different osteosyntheses treated by means of intramedullary nailing. In all cases it was considered a stable osteosynthesis, with a locking configuration which guarantee a range of local micro-movements between fracture edges compatible with callus growth.

2.1. Diffusion problem. Numerical approach

In the biological processes that control fracture healing, the concentrations of MSCs and chondrocytes at the fracture site are the trigger of the process, whereas the TNF-α and BMP-2 concentrations control the velocity of the fracture healing. The diffusion problems relating to these magnitudes must therefore be addressed to calculate the corresponding concentrations from the initial conditions.

The diffusion law employed was Fick's second law, in which the problem is governed by the following differential equation:

$$\frac{dc}{dt} = \nabla (D \nabla c) \tag{1}$$

where c is the concentration, t is the time and D is the diffusion coefficient; and ∇ is the divergence/gradient operator. If the diffusion coefficient is constant, the above equation becomes:

$$\frac{\mathrm{dc}}{\mathrm{dt}} = \mathrm{D}\ \Delta \mathrm{c} \tag{2}$$

Δ being the Laplacian operator. The boundary conditions are established as follows:

$$\partial\Omega = \Gamma_1 \cup \Gamma_2 \left\{ \begin{array}{l} \mathrm{c}\left(\vec{\mathrm{r}}, \mathrm{t}\right) = \mathscr{D}\ \Gamma_1 \ \text{(Essential conditions)} \\ \mathrm{D}\ \nabla \mathrm{c}\ \vec{\mathrm{n}} = 0\ \Gamma_2 \ \text{(Natural conditions)} \end{array} \right\} \tag{3}$$

where Γ_1 represents the part of the boundary in which the concentration is prescribed and Γ_2 represents the part of the boundary with zero flow rate (Fig. 1).

For the finite element approach, the usual method of weak formulation together with the appropriate discretization is applied. So, the reference equation becomes:

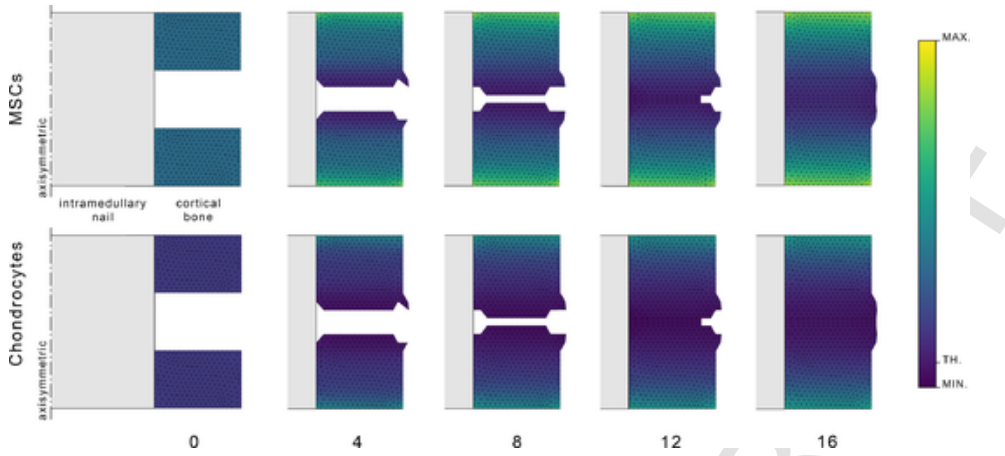

Fig. 7. Evolution of different magnitudes during the iterative process for a transverse diaphyseal femoral fracture stabilized with intramedullary nail (12 mm diameter) with an initial gap of 6 mm.

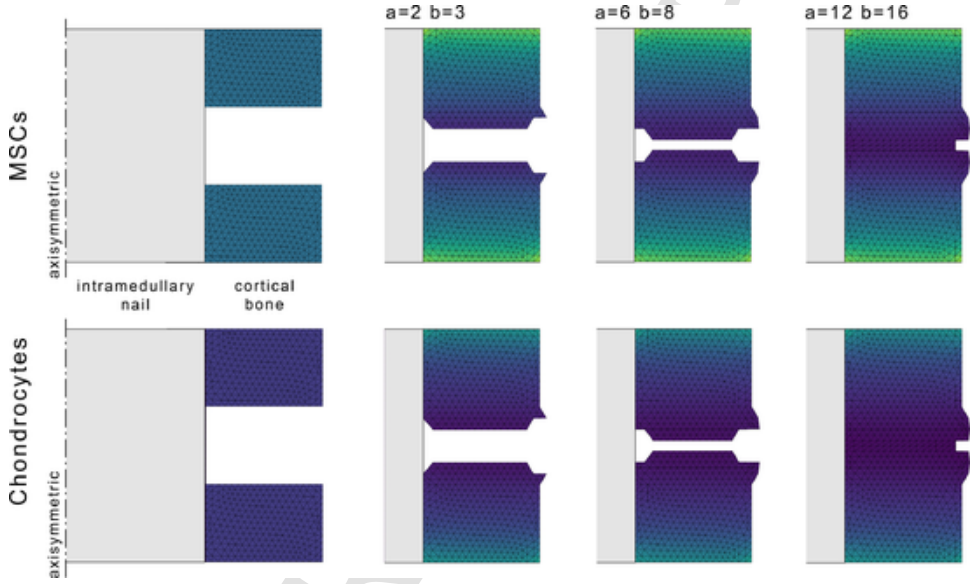

Fig. 8. Fracture healing for different callus growth velocities. The Fig. shows the same transverse fracture in the same iteration time for different values for the a and b factors of the parametric function.

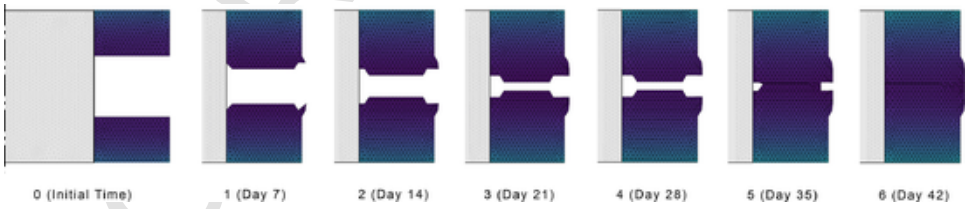

Fig. 9. Callus formation of a 4 mm gap transverse fracture with intramedullary nail fixation.

$$\sum_{e=1}^{Ne}\sum_{i=1}^{Nne}\sum_{j=1}^{Nne}\left[\frac{dc_i^e}{dt}\int_{\Omega^e}\varphi_i^e\varphi_j^e\,d\Omega^e\right] = \tag{4}$$
$$= \sum_{e=1}^{Ne}\sum_{j=1}^{Nne} D\int_{\Gamma_2^e}\varphi_j^e\,d\Gamma^e - \sum_{e=1}^{Ne}\sum_{i=1}^{Nne}\sum_{j=1}^{Nne} Dc_i^e\int_{\Omega^e}\nabla\varphi_i^e\,\nabla\varphi_j^e\,d\Omega^e$$

where c_i^e are the nodal values of concentration for each element (depending on time), $\varphi_i^e\varphi_j^e$ are the corresponding elemental approximation functions, *Ne* is the number of elements in the mesh and *Nne* is the number of nodes of the element. Using the following matrix notation:

$$\boldsymbol{M}^e = \sum_{i=1}^{Nne}\sum_{j=1}^{Nne}\int_{\Omega^e}\varphi_i^e\,\varphi_j^e\,d\Omega^e \tag{5a}$$

$$N^e = \sum_{i=1}^{Nne}\sum_{j=1}^{Nne} D\int_{\Omega^e}\nabla\varphi_i^e\,\nabla\varphi_j^e\,d\Omega^e \tag{5b}$$

$$\boldsymbol{f}^e = \sum_{j=1}^{Nne} D\int_{\Gamma_2^e}\varphi_j^e\,d\Gamma^e \tag{5c}$$

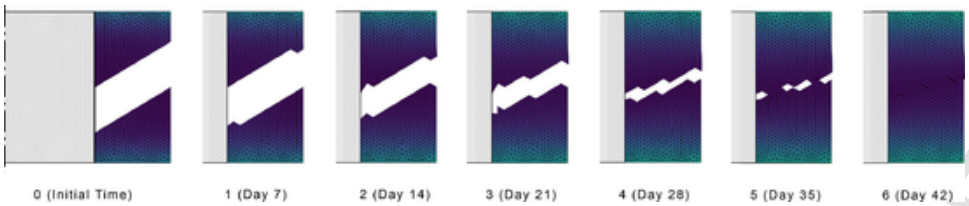

Fig. 10. Callus formation of a 3 mm 31° gap oblique fracture with intramedullary nail fixation.

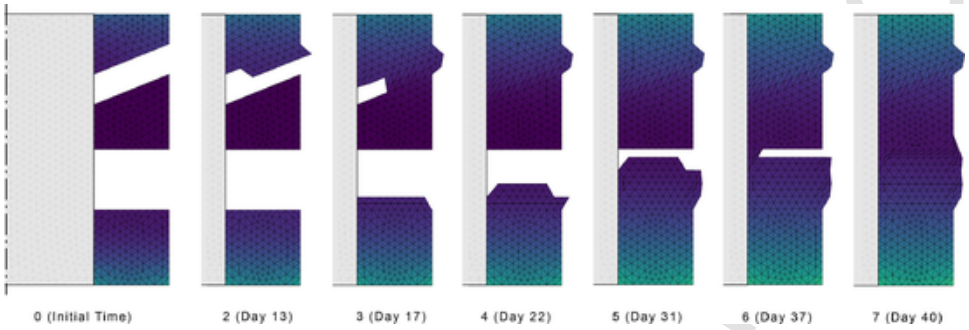

Fig. 11. Callus formation of a 2 mm 22° upper gap and 4mm lower gap of a comminuted fracture with intramedullary nail fixation.

and after assembling the different elemental matrices, the following system of differential equations is obtained:

$$\boldsymbol{M}\frac{d\boldsymbol{c}}{dt} = \boldsymbol{f} - \boldsymbol{N}\boldsymbol{c} \tag{6}$$

In order to solve the evolutionary problem defined by equation (6), a finite difference scheme is used, considering the linear approximation:

$$\boldsymbol{c}_{t+\Delta t} = \boldsymbol{c}_t + \Delta t\ \frac{d\boldsymbol{c}_t}{dt} \tag{7}$$

Then:

$$\frac{d\boldsymbol{c}_t}{dt} = \frac{\boldsymbol{c}_{t+\Delta t} - \boldsymbol{c}_t}{\Delta t} \tag{8}$$

and the iterative algorithm is established as:

$$\left(\frac{1}{\Delta t}\boldsymbol{M} + \boldsymbol{N}\right)\ \boldsymbol{c}_{t+\Delta t} = \boldsymbol{f}\ + \frac{1}{\Delta t}\ \boldsymbol{M}\ \boldsymbol{c}_t \tag{9}$$

The algorithm defined by Eq. (9) is applied to the MSCs and chondrocytes as well as the TNF-α and BMP-2 concentrations.

The solver for the diffusion problem was written in the FORTRAN language [20].

2.2. Callus growth trigger and control

Once the cell concentrations are determined for a time step along the process, a callus growth algorithm is activated depending on the previously established thresholds. The growth velocity is calculated as:

$$v = v_{max}\ \psi\ (\alpha, \beta) \tag{10}$$

with:

$$\psi\ (\alpha, \beta) = \frac{4A}{\left[1 + e^{-a(\alpha-\alpha_0)}\right]\left[1 + e^{-b(\beta-\beta_0)}\right]} + B \tag{11}$$

a normalized parametric function defined in the $[\alpha_0,1]x[\beta_0,1]$ domain. The parameters a and b are positive constants that adjust the slopes of the function and are related to the concentrations of chemical factors involved in the callus formation (in this model TNF-α and BMP-2 were used). The variables (α, β) are the dimensionless concentrations ($\alpha = c_{MSCs}/c_{MSCs}^{máx}$, $\beta = c_{cho}/c_{cho}^{máx}$), and ($\alpha_0$,$\beta_0$) are the thresholds of each concentration. Finally, A and B are adjustment constants to normalize the function as follows:

$$\begin{aligned}&\varphi\left(\alpha_0, \beta_0\right) = 0\\ &\varphi\left(1, 1\right) = 1\end{aligned} \tag{12}$$

For its part, v_{max} is chosen according to the actual physiological values corresponding to the usual healing fracture period observed in standard clinical practice [18, 21]. The defined parametric function exhibits a generalized sigmoid behaviour (Fig. 2), appropriate for different biological processes [22-24].

2.3. Callus growth algorithm

In order to proceed with the callus evolution, a growth boundary is defined. This boundary corresponds to the free faces at the fracture site, considering the normal direction to the fracture plane and an additional lateral zone at the external corners (Fig. 3). Once the concentrations are calculated and the growth velocity is determined, the possibility of growth in the corresponding step is checked. So, from the velocity and time step, the total growth volume is calculated and compared with the possible additional volume generated by the new elements added to the mesh.

The new elements grow following the normal direction of the corresponding free faces of elements which have concentrations above the corresponding thresholds. The algorithm tries to define each new element as an equilateral triangle based on the free boundary of the existing elements. For this purpose, a new node is generated at the appropriate distance from the corresponding edge, avoiding growing inside another element. In this way, a new element is generated taking as a basis the considered edge and joining it with the new node. In a second phase, the proximity between new nodes is checked, defining closing elements when appropriate. Finally, the proximity between lower and upper fronts is checked in order to proceed to the final closure of the mesh.

Some restrictions are considered in the growing algorithm. So, the algorithm does not allow the growth of an element if the angle from the normal direction to the corresponding edge is perpendicular to the natural bone axis. On the other hand, the growth is not possible if the nor-

mal direction to the corresponding edge is contrary to the determined growth direction (lower to upper or upper to lower boundary, as the case may be).

Neither can it grow if the growing element is too distorted. If the distance between the two frontiers is lower than a mesh-dependent limit, the closing algorithm starts to work. The closing algorithm finds the middle points between two free faces and then creates two new elements in the empty space. It then looks for empty spaces and fills the empty space near to the active elements (Fig. 4). A flow chart of the algorithm is shown in Fig. 5.

Once the new mesh is generated, the diffusion problem needs to be solved again for the updated model. The Python 3.8 language [25] was employed to control the workflow of the main program. A flow chart of the complete process is shown in Fig. 6.

3. Results

The proposed approach was applied to several diaphyseal femoral fractures treated by means of an intramedullary nail (a 12 mm diameter nail was considered with a bone thickness of 6 mm). Specifically, it was applied to different cases of diaphyseal femur fractures: first, a transverse fracture with an initial gap of 6 mm; second, a 3 mm 31° gap oblique fracture; and third, a 2 mm 22° upper gap and 4 mm lower gap of a comminuted fracture.

The first example corresponds to a transverse fracture with an initial gap of 6 mm. An axisymmetric local model based on triangles with quadratic approximation and an average mesh size of 1 mm was implemented. Fig. 7 shows the evolution of the MSC and chondrocyte concentrations during the iterative process.

As can be seen in the Fig., the concentrations reach the threshold values in the different elements of the growth boundary, triggering the growth process in every case.

Concerning growth velocity, the same example was used to analyse the influence of parameters a and b, depending on the TNF-α and BMP-2 concentrations. Fig. 8 shows the results for the same time step for different values of the parameters. As can be seen in the Fig., as the values of the parameters increase (higher concentrations) the callus growth velocity increases giving rise to a quicker fracture healing.

Finally, the complete approach was applied to three different types of fractures: a transverse fracture with a gap of 4.0 mm (Fig. 9), an oblique fracture with a gap of 3.0 mm and an angle of 31° (Fig. 10), and a comminuted fracture with an intermediate bone fragment with 2.0 mm for the upper gap (angle of 22°) and 4.0 mm for the lower gap (Fig. 11). All the FE models were developed with triangular quadratic elements and an average mesh size of 1.0 mm. It can be observed that the callus formation is complete in every case, despite the geometrical complexity (tilted boundary in the case of the oblique fracture; discontinuous boundary in the case of the comminuted fracture).

Moreover, in the case of the comminuted fracture the intermediate fragment was considered as devitalized, so the callus growth can only take place from upper and lower boundaries corresponding to the non-devitalized parts.

4. Discussion

A new approach for initial callus growth during fracture healing in long bones has been presented. The approach combines a diffusion model with a mesh growing algorithm that allows free growth for the callus depending on previously established conditions, without a pre-meshed domain. Mesenchymal stem cell and chondrocyte concentrations were chosen as the main biological factors controlling the callus formation, and TNF-α and the Bone Morphogenetic Protein2 as the factors influencing the velocity of the callus growth. The approach allows different biological magnitudes to be selected or changed.

Previous works on FE simulation in this field [8-15] have mainly focused on tissular differentiation and bone remodelling, considering a predefined callus form. They use a pre-meshed domain updating the type of material of the elements according to different mechanical and biological factors, but without considering the callus growth itself. None of the previously published approaches include predictive algorithms referring to the callus morphology. Moreover, the previous approaches analyse only a single biological factor, while the proposed approach simultaneously takes into account biological factors controlling callus formation as well as biological factors influencing the velocity of the callus growth.

The proposed approach was applied to several diaphyseal femoral fractures treated by means of intramedullary nailing, this being the most usual surgical technique for long bones (femur, tibia, humerus). Closed reduction followed by IM nail fixation is an ideal surgical method as it can provide strong internal fixation with a mini-incision but without interfering with local blood supply at the fracture site [26], essential for appropriate callus growth.

Three types of fractures have been included in the study. The transverse fracture model is commonly reported in different FE bone healing publications; it is therefore important to check its good performance even though transverse fractures are the least common in clinical practice. The oblique fracture is more common than the transverse, presenting greater complexity due to the angle formed with the main direction of the bone. Finally, the comminuted fracture represents an extremely complex problem, because the presence of three parts of bone and the diffusion problem concerns only to the two main bone fragments (upper and lower), the intermediate fragment being without blood supply and therefore the callus growth is only activated on the main bone fragments. No publications concerning callus growth in this type of fracture have been found.

The proposed approach has proved effective in all the analysed cases, helping us to understand the initial phase of fracture healing concerning to the callus growth in different types of fracture and under different biological conditions. Moreover, it has the advantage of natural callus growth, without the existence of a previous mesh that may affect the conditions and direction of growth.

As a main limitation of the work, it should be made clear that the proposed approach refers only to the initial phase of fracture healing, when the primary callus appears. Future work will focus on the implementation of the corresponding formulations for tissue transformation and bone remodelling in order to achieve complete fracture healing.

5. Conclusions and future work

The algorithmic strategy implemented allows the simulation of callus growth for different fracture geometry boundaries. Furthermore, the callus growth does not follow a predefined morphology of the mesh, but generates a mesh following a natural way of callus growth depending on the diffusion and growing algorithms. In consequence, there is a real generation of new mesh added to the fracture model boundaries. New elements appear in the growth boundary of the mesh, expanding the domain of the FE model. This prediction of the evolution of the callus is affected by the parametric growth function defined according to the MSC and Chondrocyte factors; at the same time the evolution reproduces the mechanism of cell colonization until the gap in the bone fracture is filled.

The algorithm accomplishes the closing of the growth boundaries, irrespective of the initial shape. The algorithm even has the ability to join isolated fragments of a comminuted fracture.

At this point, where the callus growth algorithm has been implemented and successfully tested in an axisymmetric 2D model, the research is focussing on generalizing the methodology to 3D models. In the next stage, a formulation for tissue differentiation and transforma-

tion will be developed in order to simulate bone remodelling, allowing complete fracture healing to be reproduced.

Declaration of Competing Interest

All authors state that they have no conflicts of interest.

Acknowledgement

This research was partially funded by the Spanish Ministry of Science and Innovation (DPI-201677745-R), and one FPI grant (BES-2017080433) from the University of Zaragoza obtained by José Manuel Naveiro.

References

[1] S.E. Roberts, M.J. Goldacre, Time trends and demography of mortality after fractured neck of femur in an English population, 1968-98: database study, BMJ 327 (7418) (2003 Oct) 771–775, https://doi.org/10.1136/bmj.327.7418.771.

[2] Accidents at Work By Type of Injury and Severity (NACE Rev. 2 activity A, C-N) (online data code: HSW_MI07) Source of data: Eurostat, 2021 https://ec.europa.eu/eurostat.

[3] D. Prieto-Alhambra, D. Moral-Cuesta, A. Palmer, I. Aguado-Maestro, M.F.B. Bardaji, F. Brañas, G.A. Bueno, J.R. Caeiro-Rey, I.A. Cano, M. Barres-Carsi, L.G. Delgado, M. Salomó-Domènech, I. Etxebarria-Foronda, B.L. Ferrer, S. Mills, L.E. Herrando, D. Mifsut, L.D.R. Evangelista, X. Nogués, I. Perez-Coto, J.M. Blasco, C. Martín-Hernández, H. Kessel, J.T. Serra, J.R. Solis, O.T. Suau, E. Vaquero-Cervino, C.P. Hernández, L.R. Mañas, A. Herrera, A. Díez-Perez, The impact of hip fracture on health-related quality of life and activities of daily living: the SPARE-HIP prospective cohort study, Arch. Osteoporos 14 (1) (2019) 56 May 29, https://doi.org/10.1007/s11657-019-0607-0.

[4] A. Svedbom, E. Hernlund, M. Ivergård, J. Compston, C. Cooper, J. Stenmark, E.V. McCloskey, B. Jönsson, J.A. Kanis, EU Review Panel of IOF. Osteoporosis in the European Union: a compendium of country-specific reports, Arch. Osteoporos 8 (1–2) (2013) 137 Epub 2013 Oct 11, https://doi.org/10.1007/s11657-013-0137-0.

[5] C. Cooper, G. Campion, L.J. Melton 3rd, Hip fractures in the elderly: a world-wide projection, Osteoporos. Int. (6) (1992) 285–289 Nov; 2, https://doi.org/10.1007/BF01623184.

[6] B. Hesse, A. Gächter, Complications following the treatment of trochanteric fractures with the gamma nail, Arch. Orthop. Trauma Surg. 124 (10) (2004) 692–698 Dec;doi: 10.1007/s00402-004-0744-8. Epub 2004 Oct 23.

[7] E. Madsen, M. Mededovic, D.H. Kohn, Review on material parameters to enhance bone cell function in vitro and in vivo, Biochem. Soc. Trans. 48 (5) (2020 Oct) 2039–2050, https://doi.org/10.1042/BST20200210.

[8] L.E. Claes, C.A. Heigele, Magnitudes of local stress and strain along bony surfaces predict the course and type of fracture healing, J. Biomech. 32 (3) (1999 Mar) 255–266, https://doi.org/10.1016/s0021-9290(98)00153-5.

[9] A. Bailón-Plaza, M.C. van der Meulen, A mathematical framework to study the effects of growth factor influences on fracture healing, J. Theor. Biol. 212 (2) (2001 Sep) 191–209, https://doi.org/10.1006/jtbi.2001.2372.

[10] D. Lacroix, P.J. Prendergast, A mechano-regulation model for tissue differentiation during fracture healing: analysis of gap size and loading, J. Biomech. 35 (9) (2002 Sep) 1163–1171, https://doi.org/10.1016/s0021-9290(02)00086-6.

[11] U. Simon, P. Augat, M. Utz, L. Claes, A numerical model of the fracture healing process that describes tissue development and revascularisation, Comput. Methods Biomech. Biomed. Eng. 14 (1) (2011) 79–93 10.1080/10255842.2010.499865. Epub 2010 Nov 1.

[12] S.J. Shefelbine, P. Augat, L. Claes, U. Simon, Trabecular bone fracture healing simulation with finite element analysis and fuzzy logic, J. Biomech. 38 (12) (2005 Dec) 2440–2450 Epub 2005 Jan 6, https://doi.org/10.1016/j.jbiomech.2004.10.019.

[13] C.J. Wilson, M.A. Schütz, D.R. Epari, Computational simulation of bone fracture healing under inverse dynamisation, Biomech. Model. Mechanobiol. 16 (1) (2017) 5–14 Feb10.1007/s10237-016-0798-x. Epub 2016 May 24.

[14] M. Wang, N. Yang, Three-dimensional computational model simulating the fracture healing process with both biphasic poroelastic finite element analysis and fuzzy logic control, Sci. Rep. 8 (1) (2018 Apr) 6744, https://doi.org/10.1038/s41598-018-25229-7.

[15] M. Wang, N. Yang, X. Wang, A review of computational models of bone fracture healing, Med. Biol. Eng. Comput. 55 (11) (2017 Nov) 1895–1914 10.1007/s11517-017-1701-3. Epub 2017 Aug 8.

[16] J.E. Dennis, A.I. Caplan, Bone marrow mesenchymal stem cells In: Sell S. (eds) Stem Cells Handbook, Humana Press, Totowa, NJ, 2004, https://doi.org/10.1007/978-1-59259-411-5_10.

[17] D. Zi-chuan, L. Yi-kai, G. Yao-kai, Molecular pathogenesis of fracture nonunion, J. Orthopaedic Translat. 14 (2018) 45–56, https://doi.org/10.1016/j.jot.2018.05.002.

[18] R. Marsell, T.A. Einhorn, The biology of fracture healing. Injury, Int. J. Care Injured. 42 (6) (2011) 551–555 Epub 2011 Apr 13, https://doi.org/10.1016/j.injury.2011.03.031.

[19] A. Nautha, J. Ristiniemi, Bone morphogenetic proteins in open fractures: past, present, and future. Injury, Int. J. Care Injured. 40 (S3) (2009) S27–S31, https://doi.org/10.1016/S0020-1383(09)70008-7.

[20] gfortran-the GNU Fortran compiler, part of GCC, version 8. Available at https://gcc.gnu.org/wiki/GFortranBinaries, 2021.

[21] T.A. Einhorn, L.C. Gerstenfeld, Fracture healing: mechanisms and interventions, Nat. Rev. Rheumatol. 11 (1) (2015) 45–54 JanEpub 2014 Sep 30, https://doi.org/10.1038/nrrheum.2014.164.

[22] S. Mouloodi, H. Rahmanpanah, C. Burvill, H.M.S. Davies, Prediction of load in a long bone using an artificial neural network prediction algorithm, J. Mech. Behav. Biomed. Mater. 102 (2020) FebEpub 2019 Nov 11 103527, https://doi.org/10.1016/j.jmbbm.2019.103527.

[23] F. Piccialli, V. Di Somma, F. Giampaolo, S. Cuomo, G. Fortino, A survey on deep learning in medicine: why, how and when?, Informat. Fusion 66 (2021) 111–137 doi:, https://doi.org/10.1016/j.inffus.2020.09.006.

[24] R. Hambli, H. Katerchi, C.L. Benhamou, Multiscale methodology for bone remodelling simulation using coupled finite element and neural network computation, Biomech. Model. Mechanobiol. 10 (1) (2011) 133–145 Febdoi: 10.1007/s10237-010-0222-x. Epub 2010 May 27.

[25] Python Software Foundation. Python Language Reference, version 3.8. Available at http://www.python.org

[26] R.A. Winquist, Locked femoral nailing, J. Am. Acad. Orthop. Surg. 1 (2) (1993 Nov) 95–105 doi:, https://doi.org/10.5435/00124635-199311000-00004.